Biomagnetic Steady Flow through an Axisymmetric Stenosed Artery

Manish Gaur and Manoj Kumar Gupta

Department of Mathematics,
Government College, Kota,
Rajasthan – 324001, India

ABSTRACT: The steady slip flow assuming blood as the Casson fluid has been studied under the influence of transverse magnetic field. The results for the axial velocity, plug flow velocity, flow flux and the wall shear stress have been analyzed analytically and graphically taking suitable parameters. The analysis shows that the axial velocity, plug flow velocity and the flow flux increase along axial distance as the pressure gradient, magnetic field gradient and slip velocity increase but they decrease when the stenosis height increases. Also the wall shear stress showing fluctuations increase in z – direction when the pressure gradients, magnetic field gradient, slip velocity and the stenosis height increase. It also increases radially when magnetic field gradient increases but it decreases when the slip velocity increases.

KEYWORDS: Casson Fluid; Constricted Artery; Slip Boundary Condition; Yield Stress, Magnetic Flow.

1   INTRODUCTION

Many medical research works have so far proved this fact that the narrowing of the blood vessels is causing serious disorders in blood circulations which sometimes lead to the heart failures. It has been observed that the initial deposits of lipids at the sub-endothelial space and then extra addition of macrophages become fibrous in due course of time which creates the cardiovascular problems. So far a number of mathematical models taking different blood features have been proposed to study the rheology of blood. The magnetic aspect of blood has always been an interesting topic of research for the research workers. Since the hemoglobin present in the mature blood cells is a form of iron-oxides, therefore the blood behaves as a biomagnetic fluid. Some research workers have worked on the magnetic property of blood flow under stenotic conditions.

D.F. Young [1] studied the effect of an axially symmetric time-dependent stenotic growth into the lumen of a tube of constant cross-section over the steady flow by taking the blood as a Newtonian fluid. P.K. Suri et al. [2] presented a mathematical simulation of blood flow through branched arteries under transverse magnetic field and observed that the applied magnetic field reduces the strength of blockage at the apex of bifurcation. J.C. Mishra et al. [3] studied the flow through stenosed arteries. J.C. Mishra et al. [4] used the momentum integral method to study flow characteristic of blood through stenosed vessel. K. Haldar et al. [5] studied the effect of magnetic field on blood flow through indented tube in the presence of erythrocytes. V. P. Srivastava [6] dealt with the problem of stenotic blood flow taking blood as a particle-fluid suspension model and observed that the magnitudes of blood flow characteristics significantly increase with increase in red cell concentration. H.P. Mazumdar et al. [7] investigated some flow characteristics of a Newtonian fluid under effect of magnetic field through a circular tube.

Y. Haik et al. [8] studied the apparent additive viscosity of human blood because of a high static magnetic field and showed that the blood flow under gravity reduces by 30% when it is kept under high magnetic field of 10 T. J.C. Mishra et al. [9] gave a numerical model to study the effect of magnetic field on blood flow through an artery. S. Kenjeres [10] analyzed blood flow numerically in realistic arteries subjected to strong non-uniform magnetic fields. L. Parmar et al. [11] investigated the role of magnetic field intensity in Herschel – Bulkley blood flow through overlapping stenosed artery. Gaur and Gupta

[12] discussed a Casson fluid model to study the steady flow through a stenosed blood vessel in which the authors explained that the axial velocity, volumetric flow rate and pressure gradient increase with the increase in slip velocity and decrease with growth in yield stress. Gaur and Gupta [13] also studied the slip effects on steady flow through a stenosed blood artery and found that axial velocity, volumetric flow rate and pressure gradient decrease along the radial distance as the slip length increases but the wall shear stress increases with increase in slip length.

2   MATHEMATICAL FORMULATION

Let the blood flow be steady, laminar and incompressible through an axially symmetric stenosed cylindrical artery in z − direction.

The geometrical diagram of the stenosed artery is given below:
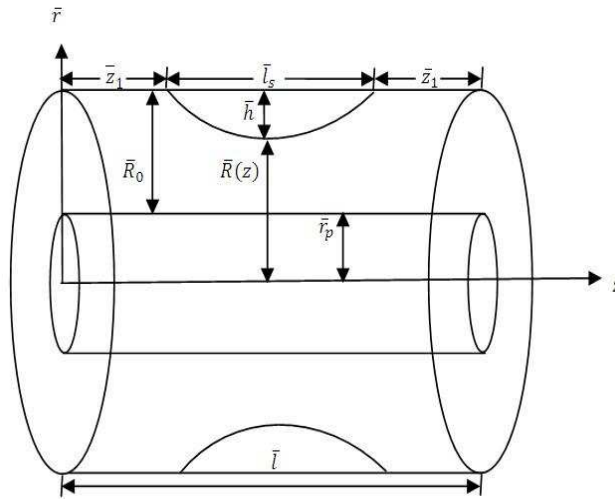
Let $\bar{R}_0$ be the radius of the normal tube and $\bar{R}(\bar{z})$ is the radius of the constricted area given by (Young, 1968):

$$\bar{R}(\bar{z}) = \begin{cases} \bar{R}_0 - \frac{\bar{h}}{2}\left[1 + \cos\frac{2\pi}{\bar{l}_s}\left(\bar{z}_1 + \bar{l}_s - \bar{z}\right)\right]; & \bar{z}_1 \leq \bar{z} \leq \bar{z}_1 + \bar{l}_s \\ \bar{R}_0 & ; \text{ otherwise} \end{cases} \tag{2.1}$$

Where $\bar{l}_s$ is the length of the stenosis in the artery of the length $\bar{l}$, $\bar{z}_1$ is the location of the stenosis of maximum height $\bar{h}$. Also, let $\bar{r}$ and $\bar{z}$ be radial and axial coordinates.

Here the blood is considered to behave as a Casson fluid under the effect of an externally applied uniform transverse magnetic field which generates a motion due to which the fluid particles are attracted towards the magnetic field.

Under the above considerations, the equations of motion in the dimensional form are:

$$-\frac{\partial \bar{p}}{\partial \bar{z}} + \frac{1}{\bar{r}}\frac{\partial}{\partial \bar{r}}(\bar{r}\bar{\tau}_c) + \in_0 M\frac{\partial \bar{B}}{\partial \bar{z}} = 0 \tag{2.2}$$

$$\frac{\partial \bar{p}}{\partial \bar{r}} = 0 \tag{2.3}$$

Where $\bar{p}$ denotes pressure at any point, $\in_0$ magnetic permeability, M magnetization and $\bar{B}$ represents the magnetic field intensity. Also $\bar{\tau}_c$ denotes the shear stress of the fluid. Casson fluid has the following simplified constitutive equations:

$$F(\bar{\tau}_c) = -\frac{\partial \bar{v}_c}{\partial \bar{r}} = \frac{1}{\bar{k}_c}\left(\bar{\tau}_c^{1/2} - \bar{\tau}_0^{1/2}\right)^2 \text{ for } \bar{\tau}_c \geq \bar{\tau}_0 \tag{2.4}$$

$$\frac{\partial \bar{v}_c}{\partial \bar{r}} = 0 \qquad \text{ for } \bar{\tau}_c \leq \bar{\tau}_0 \tag{2.5}$$

where $\bar{v}_c$ is the axial velocity of the blood, $\bar{\tau}_0$ represents the yield stress and $\bar{k}_c$ is the fluid viscosity.

The equations (2.2) to (2.5) are subject to the following boundary conditions:

$$\left.\begin{array}{ll} \bar{v}_c = \bar{v}_s & \text{at } \bar{r} = \bar{R}(\bar{z}) \\ \bar{\tau}_c = \text{Finite value} & \text{at } \bar{r} = 0 \end{array}\right\}$$

(2.6)

where $\bar{v}_s$ denotes the slip velocity along z – axis.

Let us introduce the following non – dimensional variables as

$$R(z) = \frac{\bar{R}(\bar{z})}{\bar{R}_0}, \quad z = \frac{\bar{z}_1 + \bar{l}_s - \bar{z}}{\bar{l}_s}, \quad r = \frac{\bar{r}}{\bar{R}_0}, \quad \tau_c = \frac{\bar{\tau}_c}{\bar{p}_0 \bar{R}_0/2}, \quad \tau_0 = \frac{\bar{\tau}_0}{\bar{p}_0 \bar{R}_0/2}, \quad v_c = \frac{\bar{v}_c}{\bar{p}_0 \bar{R}_0^2/2\bar{k}_c}, \quad v_s = \frac{\bar{v}_s}{\bar{p}_0 \bar{R}_0^2/2\bar{k}_c},$$

$$H = \frac{\bar{h}}{\bar{R}_0}, \quad B = \frac{\bar{B}}{\bar{B}_0}, \quad \frac{\partial p}{\partial z} = \frac{\partial \bar{p}/\partial \bar{z}}{\bar{p}_0}$$

(2.7)

Here $\bar{p}_0$ is the steady – state amplitude and $\bar{B}_0$ represents the external transverse uniform constant magnetic field.

Under the above non – dimensional conditions, the radius of the stenotic area of the artery becomes

$$R(z) = \begin{cases} 1 - H\cos^2 \pi z; & 0 \le z \le 1 \\ 1 & ; \text{ otherwise} \end{cases}$$

(2.8)

The dimensionless forms of equations (2.2) to (2.5) are

$$-2\frac{\partial p}{\partial z} + \frac{1}{r}\frac{\partial}{\partial r}(r\tau_c) - C\frac{\partial B}{\partial z} = 0$$

(2.9)

$$\frac{\partial p}{\partial r} = 0$$

(2.10)

$$-\frac{\partial v_c}{\partial r} = (\tau_c^{1/2} - \tau_0^{1/2})^2 \qquad \text{for } \tau_c \ge \tau_0$$

(2.11)

$$\frac{\partial v_c}{\partial r} = 0 \qquad\qquad \text{for } \tau_c \le \tau_0$$

(2.12)

where $C = \frac{2\epsilon_0 M\bar{B}_0}{\bar{p}_0 \bar{l}_s}$

(2.13)

The non – dimensional boundary conditions are

$$\left.\begin{array}{ll} v_c = v_s & \text{at } r = R(z) \\ \tau_c = \text{Finite value} & \text{at } \bar{r} = 0 \end{array}\right\}$$

(2.14)

Using condition (2.14) in equation (2.9), the shear stress τ_c and wall shear stress τ_R can be written as

$$\tau_c = \frac{r}{2}\left(2\frac{\partial p}{\partial z} + C\frac{\partial B}{\partial z}\right)$$

(2.15)

$$\tau_R = \frac{R}{2}\left(2\frac{\partial p}{\partial z} + C\frac{\partial B}{\partial z}\right)$$

(2.16)

From equations (2.14) and (2.15),

$$\frac{\tau_c}{\tau_R} = \frac{r}{R}$$

(2.17)

3   METHOD OF SOLUTION

Thus velocity in the region $r_p \leq r \leq R(z)$ is obtained by integrating equation (2.11) using conditions (2.14) and (2.15) where $r_p = \frac{\bar{r}_p}{\bar{R}_0}$ is the non – dimensional radius of the plug flow region, given as

$$v_c = v_s + \frac{1}{\left(2\frac{\partial p}{\partial z}+c\frac{\partial B}{\partial z}\right)}\left[\left(\tau_R^{1/2} - \tau_0^{1/2}\right)^4 + \frac{4}{3}\tau_0^{1/2}\left(\tau_R^{1/2} - \tau_0^{1/2}\right)^3 - \left(\tau_c^{1/2} - \tau_0^{1/2}\right)^4 - \frac{4}{3}\tau_0^{1/2}\left(\tau_c^{1/2} - \tau_0^{1/2}\right)^3\right] \tag{3.1}$$

Within plug flow region i.e. $0 \leq r \leq r_p$, $\tau_c = \tau_0$ at $r = r_p$, therefore the plug flow velocity is

$$v_c = v_s + \frac{1}{\left(2\frac{\partial p}{\partial z}+c\frac{\partial B}{\partial z}\right)}\left[\left(\tau_R^{1/2} - \tau_0^{1/2}\right)^4 + \frac{4}{3}\tau_0^{1/2}\left(\tau_R^{1/2} - \tau_0^{1/2}\right)^3\right] \tag{3.2}$$

Now the volumetric flow rate in the dimensionless form for the region $0 \leq r \leq R(z)$ can be obtained as

$$Q = 4\int_0^R rv(r)dr$$

$$= 4\int_0^{r_p} rv_p dr + 4\int_{r_p}^R rv_c dr$$

Hence

$$Q = 2R^2 v_s + \frac{R^2}{\left(2\frac{\partial p}{\partial z}+c\frac{\partial B}{\partial z}\right)}\left[2\left(\tau_R^{1/2} - \tau_0^{1/2}\right)^4 + \frac{4}{3}\tau_0^{1/2}\left(\tau_R^{1/2} - \tau_0^{1/2}\right)^3\right] + \frac{R^2}{\left(2\frac{\partial p}{\partial z}+C\frac{\partial B}{\partial z}\right)\tau_R^2}\left[\tau_R^4 - \frac{2}{3}\tau_R^2\tau_0^2 + \frac{8}{3}\tau_R^3\tau_0 - \frac{64}{21}\tau_R^{7/2}\tau_0^{1/2} + \frac{1}{21}\tau_0^4\right] \tag{3.3}$$

If $\tau_0 \ll \tau_R$ i.e. $\frac{\tau_0}{\tau_R} \ll 1$, then equation (3.3) reduces to the form

$$Q = 2R^2 v_s + \frac{R^2 \tau_R}{\left(2\frac{\partial p}{\partial z}+C\frac{\partial B}{\partial z}\right)}\left(\tau_R - \frac{16}{7}\tau_0^{1/2}\tau_R^{1/2} + \frac{4}{3}\tau_0\right) \tag{3.4}$$

which also gives us the wall shear stress for the stenosed artery as

$$\tau_R = \left[\frac{8}{7}\tau_0^{1/2} + \left\{\frac{r(Q-2R^2 v_s)}{R^3 \tau_c}\left(2\frac{\partial p}{\partial z} + C\frac{\partial B}{\partial z}\right) - \frac{4}{147}\tau_0\right\}^{1/2}\right]^2 \tag{3.5}$$

If there is no stenosis i.e. $R(z) = R_0$ then the wall shear stress for the non – constricted artery is given as

$$\tau_N = \left[\frac{8}{7}\tau_0^{1/2} + \left\{\frac{r(Q-2R_0^2 v_s)}{R_0^3 \tau_c}\left(2\frac{\partial p}{\partial z} + C\frac{\partial B}{\partial z}\right) - \frac{4}{147}\tau_0\right\}^{1/2}\right]^2 \tag{3.6}$$

4   RESULTS AND DISCUSSION

The velocity profile for the axial velocity in the non – plug flow region has been obtained in equation (3.1) and the graphical discussions of the results are given in figures 1(a) and 1(b).

	τ_0	H	$\partial p/\partial z$	$\partial B/\partial z$	v_s
I	0.010	0.10	0.5	0.10×10^4	0.5
II	0.020	0.10	0.5	0.10×10^4	0.5
III	0.010	0.15	0.5	0.10×10^4	0.5
IV	0.010	0.10	1.0	0.10×10^4	0.5
V	0.010	0.10	0.5	0.11×10^4	0.5
VI	0.010	0.10	0.5	0.10×10^4	1.0
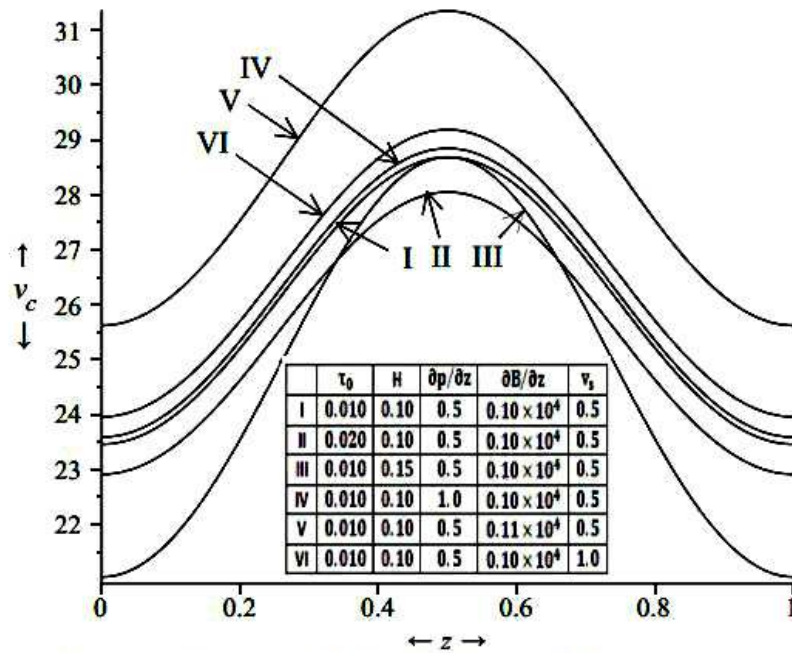
Figure 1 (a): Variation of Axial Velocity Along Axial Distance for Different Values of the Stenosis Height H, pressure gradient $\frac{\partial p}{\partial z}$, Magnetic Field Gradient $\frac{\partial B}{\partial z}$, Yield Stress τ_0 and Slip Velocity v_s.

Figure 1(a) gives the variations of the axial velocity versus axial distance for the different values of the stenosis height H, pressure gradient $\frac{\partial p}{\partial z}$, magnetic field gradient $\frac{\partial B}{\partial z}$, yield stress τ_0 and slip velocity v_s with some fixed value $\tau_c = 0.030$. It is observed that the axial velocity first increases achieving a maximum value at the peak of the stenosis and then starts decreasing along the axial distance. Also the axial velocity increases with an increase in slip velocity, pressure gradient and magnetic field gradient but it decreases when the yield stress increases.

	τ_0	$\partial B/\partial z$	v_s
I	0.010	0.10×10^4	0.5
II	0.020	0.10×10^4	0.5
III	0.010	0.11×10^4	0.5
IV	0.010	0.10×10^4	1.0
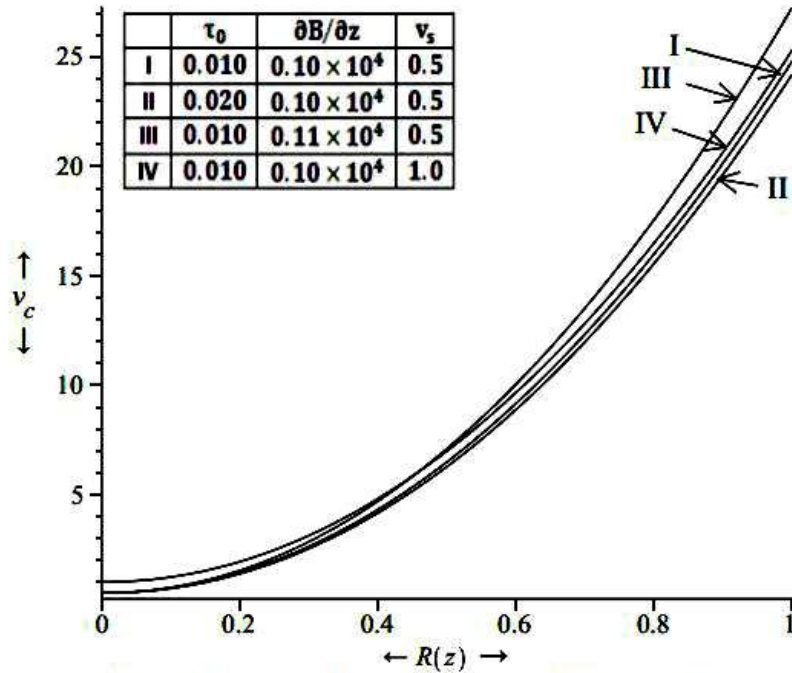
Figure 1 (b): Variation of Axial Velocity Along Radial Distance for Different Values of the Magnetic Field Gradient $\frac{\partial B}{\partial z}$, Yield Stress τ_0 and Slip Velocity v_s.

Figure 1(b) shows the variations of the axial velocity along radial distance for the various values of the magnetic field gradient $\frac{\partial B}{\partial z}$, yield stress τ_0 and slip velocity v_s with some fixed value $\tau_c = 0.030$. When the magnetic field increases, the axial velocity starts increasing slowly but it increases fast as the radial distance increases. As the slip velocity increases, the axial velocity increases a little fast but grows slowly when the radial distance increases. The axial velocity decreases slowly when the yield stress increases along the radial distance.

The graphical description of the axial velocity for the plug flow area obtained through equation (3.2) has been given in figures 2(a) and 2(b).
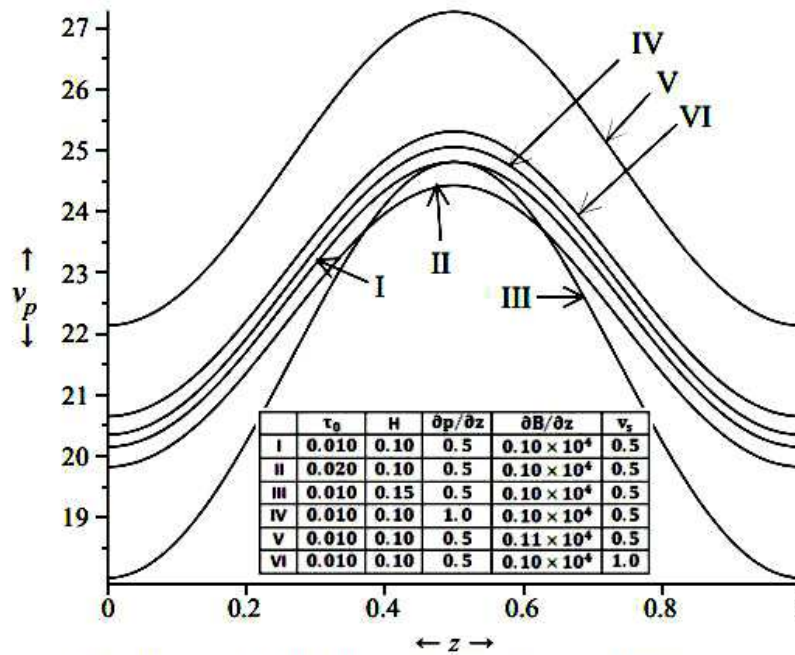
Figure 2(a): Variation of Plug Flow Velocity Along Axial Distance for Different Values of the Stenosis Height H, pressure gradient $\frac{\partial p}{\partial z}$, Magnetic Field Gradient $\frac{\partial B}{\partial z}$, Yield Stress τ_0 and Slip Velocity v_s.

Figure 2(a) describes the changes in plug flow velocity along axial distance for the different values of the stenosis height H, pressure gradient $\frac{\partial p}{\partial z}$, magnetic field gradient $\frac{\partial B}{\partial z}$, yield stress τ_0 and slip velocity v_s with a fixed value $\tau_c = 0.030$. The graph shows that the plug flow velocity first increases to get a maximum value at the peak of the stenosis along the axial distance and after a certain point it starts decreasing. The plug flow velocity increases greatly for smaller increments in magnetic field gradient along the axial distance. As the slip velocity increases, the plug flow velocity increases with pulse along the axial distance. When the pressure gradient increases, the plug flow velocity increases along the z – axis. The plug flow velocity deceases as the yield stress increases.

Figure 2 (b): Variation of Plug Flow Velocity Along Radial Distance for Different Values of the Magnetic Field Gradient $\dfrac{\partial B}{\partial z}$, Yield Stress τ_0 and Slip Velocity v_s.

Figure 2(b) shows the variations in plug flow velocity versus radial distance for the different values of the pressure gradient $\frac{\partial p}{\partial z}$, magnetic field gradient $\frac{\partial B}{\partial z}$, yield stress τ_0 and slip velocity v_s with some fixed value $\tau_c = 0.030$. It clarifies that the plug flow velocity increases along the radial distance. As the magnetic field gradient increases, the plug flow velocity increases very slowly for smaller radial distance but it increases fast as the radial distance increases. When the slip velocity increases, the pug flow velocity increases fast for lower radial distance but it becomes slower along the radial distance. Also the plug flow velocity decreases as the yield stress increases.
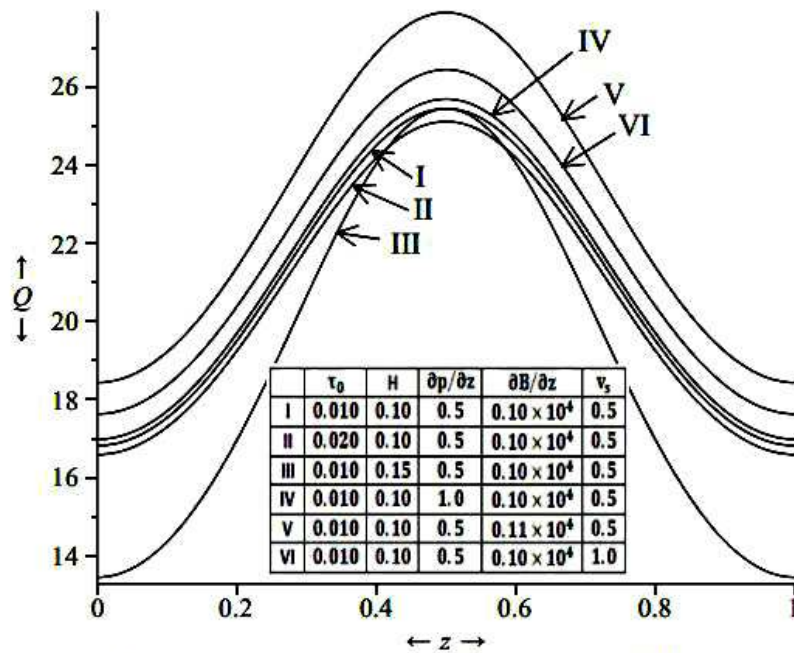
Figure 3(a): Variation of Volumetric Flow Rate Along Axial Distance for Different Values of the Stenosis Height H, pressure gradient $\frac{\partial p}{\partial z}$, Magnetic Field Gradient $\frac{\partial B}{\partial z}$, Yield Stress τ_0 and Slip Velocity v_s.

The variations of the volumetric flow rate obtained through equation (3.4) are shown along the axial distance for the various values of the stenosis height H, pressure gradient $\frac{\partial p}{\partial z}$, magnetic field gradient $\frac{\partial B}{\partial z}$ and slip velocity v_s with a fixed value $\tau_c = 0.030$ in figure 3(a). It shows that the flow flux first increases and after getting a maximum value the peak of the stenosis, it decreases. When the pressure gradient increases, the volumetric flow rate increases slowly with pulse along the axial distance. As slip velocity increases, the flow flux increases fast. The flow flux increases greatly for smaller increments in the magnetic field gradient along the axial distance. The volumetric flow rate decreases slowly with increment in the yield stress along the axial distance.
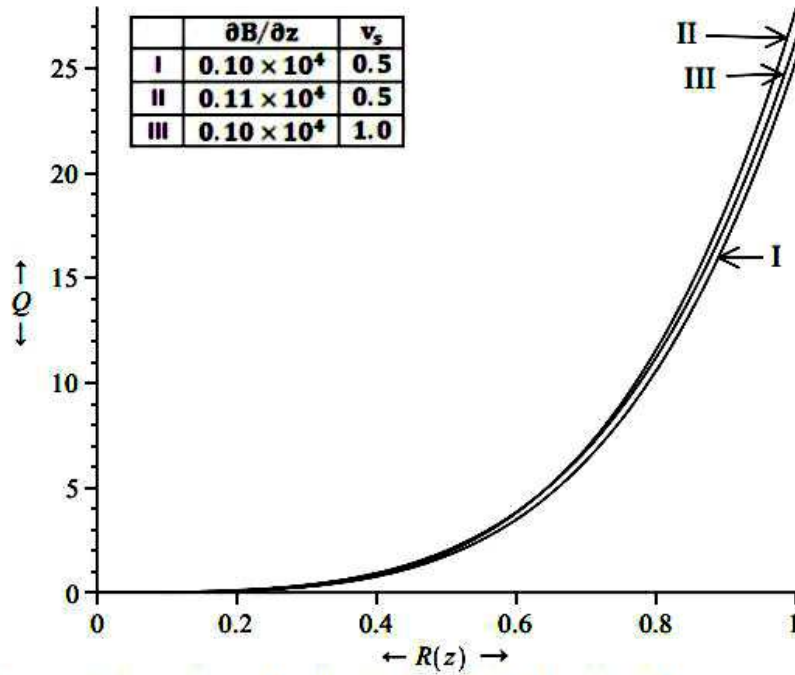
Figure 3 (b): Variation of Volumetric Flow Rate Along Radial Distance for Different Values of the Magnetic Field Gradient $\frac{\partial B}{\partial z}$ and Slip Velocity v_s.

Figure 3(b) shows the changes in the volumetric flow rate along the radial distance for the different values of the magnetic field gradient $\frac{\partial B}{\partial z}$ and slip velocity v_s with a fixed value $\tau_c = 0.030$. The volumetric flow rate keeps on growing along the radial distance. The flow flux increases very slowly for smaller increments in the magnetic field gradient along the radial distance. When the slip velocity increases, the volumetric flow rate increases slowly for lower radial distance but it increases fast as the radial distance increases.

	H	∂p/∂z	∂B/∂z	v_s
I	0.10	0.5	0.10×10^4	0.5
II	0.15	0.5	0.10×10^4	0.5
III	0.10	1.0	0.10×10^4	0.5
IV	0.10	0.5	0.11×10^4	0.5
V	0.10	0.5	0.10×10^4	0.4
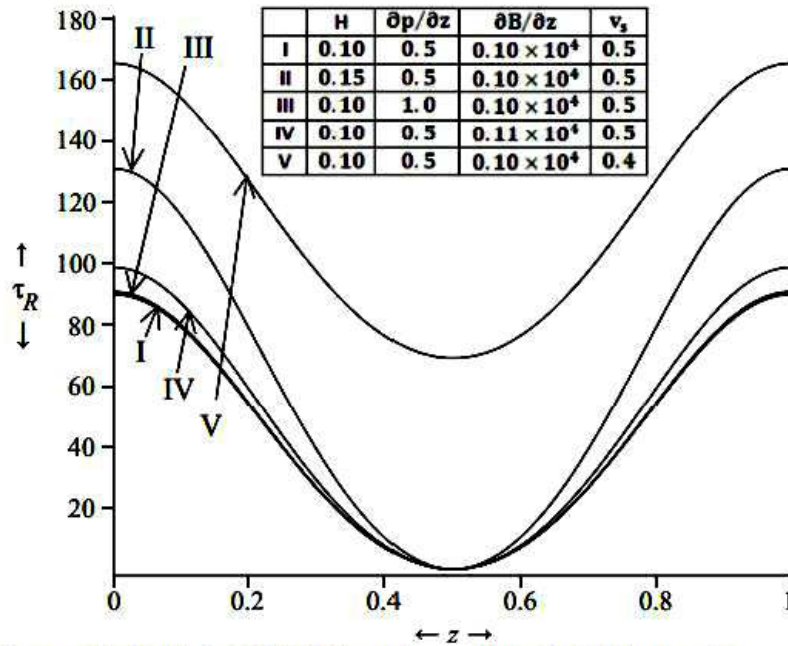
Figure 4 (a): Variation of Wall Shear Stress Along Axial Distance for Different Values of the Stenosis Height H, pressure gradient $\frac{\partial p}{\partial z}$, Magnetic Field Gradient $\frac{\partial B}{\partial z}$ and Slip Velocity v_s.

Figure 4(a) shows the variations of the wall shear stress derived through equation (3.5) along the axial distance for the different values of the stenosis height H, pressure gradient $\frac{\partial p}{\partial z}$, magnetic field gradient $\frac{\partial B}{\partial z}$ and slip velocity v_s with a fixed value $\tau_c = 0.030$. The wall shear stress keeps on changing from high value to low value at the peak of the stenosis and then again to high value along the axial distance. When the pressure gradient increases, the wall shear stress increases very slowly along the axial distance. It almost coincides with the previous values of the wall shear stress. With increase in the magnetic field gradient, the wall shear stress increases. As the slip velocity increases, the wall shear stress increases greatly along the axial distance.
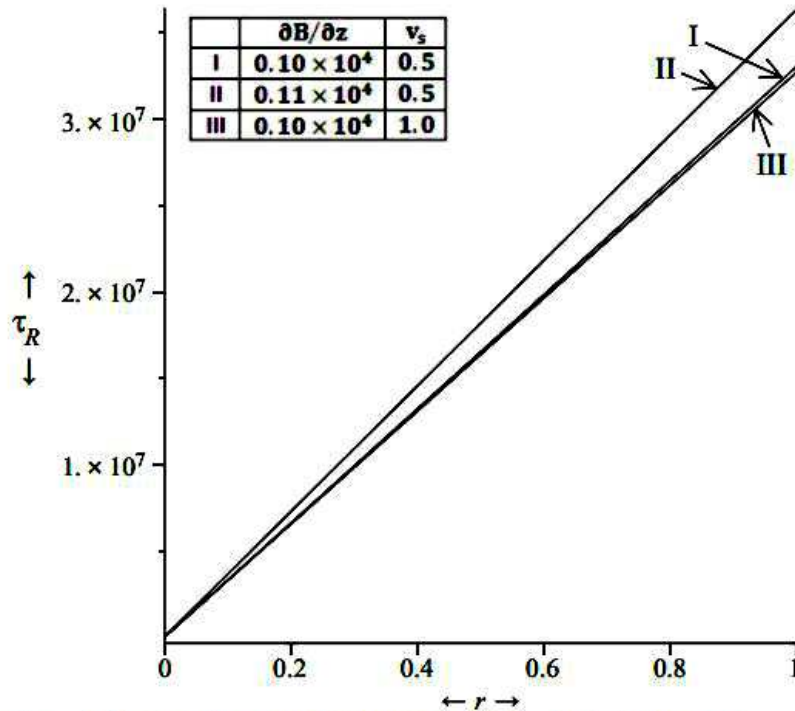
Figure 4 (b): Variation of Wall Shear Stress Along Radial Distance for Different Values of the Magnetic Field Gradient $\frac{\partial B}{\partial z}$ and Slip Velocity v_s.

Figure 4(b) gives the changes in the wall shear stress versus the radial distance for the different values of the magnetic field gradient $\frac{\partial B}{\partial z}$ and slip velocity v_s with a fixed value $\tau_c = 0.030$. It is clear that the wall shear stress increases fast along the radial distance when the magnetic field gradient increases. Also the wall shear stress very slowly along the radial distance as the slip velocity increases.

The graphical representations of variations of some flow characteristics were not very clear due to the very small changes in the corresponding values. Therefore these variations are provided in tabulated forms.

Table 1: Variation of Fluid Velocity in Plug Flow and Non-plug Flow Regions versus Pressure Gradient Along Radial Distance.

$\frac{\partial p}{\partial z}$	$R(z) = 0.0$		$R(z) = 0.5$		$R(z) = 1.0$	
	v_c	v_p	v_c	v_p	v_c	v_p
0.5	0.4999988678	0.4999996700	6.482503006	6.482503808	24.81248750	24.81248830
1.0	0.4999988788	0.4999996732	6.543348722	6.543349516	25.05780843	25.05780922
1.5	0.4999988897	0.4999996764	6.604202524	6.604203310	25.30315227	25.30315306

The variations of axial and plug flow velocities versus pressure gradient along the radial distance are given in Table 1. It is clear from the table that the fluid velocities in both plug flow and non – plug flow regions is increasing with increase in the pressure gradient along the radial distance. The fluid velocity is also increasing when it enters from non – plug flow region to the plug flow region.

Table 2(a): Variations of Volumetric Flow Rate versus Pressure Gradient Along Radial Distance.

$\frac{\partial p}{\partial z}$	Q		
	$R = 0.0$	$R = 0.5$	$R = 1.0$
0.5	0.0	1.757173507	25.44451407
1.0	0.0	1.772444012	25.69050341
1.5	0.0	1.787716250	25.93651237

Table 2(a) shows the variations of the volumetric flow rate versus pressure gradient along the radial distance. When the pressure gradient increases, the flow flux increases along the radial distance.

Table 2(b): Variations of Volumetric Flow Rate versus Yield Stress Along Radial Distance.

τ_0	Q		
	$R = 0.0$	$R = 0.5$	$R = 1.0$
0.010	0.0	1.757173507	25.44451407
0.015	0.0	1.728272593	25.11477613
0.020	0.0	1.706290034	24.86331044

Table 2(b) gives the changes in the volumetric flow rate versus pressure gradient along the radial distance. It is observed that the flow flux increases along the radial distance as the yield stress increase.

Table 3(a): Variations of Wall Shear Stress versus Yield Stress Along Axial and Radial Distance.

τ_0	τ_R					
	z			r		
	0.1	0.4	1.0	0.1	0.4	1.0
0.010	79.301771	7.185297	89.899646	3.3037154×10^6	1.3214030×10^7	3.3034313×10^7
0.015	79.759752	7.323514	90.387237	3.3038088×10^6	1.3214217×10^7	3.3034608×10^7
0.020	80.146851	7.441036	90.799298	3.3038875×10^6	1.3214375×10^7	3.3034857×10^7

The variations of the wall shear stress along axial and radial distances for different values of the yield stress are given in Table 3(a). The wall shear stress first decreases and after a minimum values it again starts increasing along axial distance with increase in the yield stress. The wall stress also increases along the radial distance when the yield stress increases.

Table 3(b): Variations of Wall Shear Stress versus Yield Stress Along Axial and Radial Distance.

$\dfrac{\partial p}{\partial z}$	τ_R		
	$r = 0.1$	$r = 0.4$	$r = 1.0$
0.5	3.303715444×10^6	1.321403087×10^7	3.303431371×10^7
1.0	3.307015649×10^6	1.322723129×10^7	3.306731437×10^7
1.5	3.310315856×10^6	1.324043170×10^7	3.310031503×10^7

Table 3(b) exhibits the changes in the wall shear stress versus pressure gradient along the radial distance. It is obvious that the wall shear stress increases along the radial distance when the pressure gradient increases.

5 CONCLUSION

The present model deals with the study of the magnetic feature of blood as a Casson fluid. The values of the different parameters used in the analysis have been taken from the work [11.] The analysis of the study shows that the volumetric flow rate and the axial velocity increase along axial distance with pulse when the axial distance, pressure gradient, magnetic field gradient, yield stress and slip velocity increase and the axial velocity in plug flow region along radial distance decreases when yield stress increases but it rises with increase in magnetic field gradient and slip velocity. The axial velocity in both plug and non – plug flow regions and the flow flux decrease along the axial distance with increase in stenosis height. The axial and the plug flow velocity increase with increase in the pressure gradient along the radial distance. The flow flux in radial direction increases when the magnetic field gradient, pressure gradient and the slip velocity increase. The wall shear stress shows fluctuations along the axial distance from higher values to the minimum value and then again to higher values. It increases as the pressure gradient, magnetic field gradient, slip velocity and stenosis height increase in z – direction. Also the wall shear stress increases when magnetic field gradient increases but it decreases as the slip velocity increases. The wall shear stress increases along radial distance with increase in pressure gradient and the yield stress.

REFERENCES

[1] D. F. Young, "Effect of time dependent stenosis on flow through a tube", *J. Engg. For Ind., Trans of ASME*, 90, pp. 248–254, 1968.

[2] P. K. Suri and R. Pushpa, "Effect of static magnetic field on blood flow in a branch", *J. Pure and Appl. Math.*, Vol. 12, No. 7, pp. 907–918, 1981.

[3] J. C. Mishra and S. Chakravorty, "Flow in arteries in the presence of stenosis", *J. Biomech.*, Vol. 19, No. 11, 1986, pp. 1907–1918, 1986.

[4] J. C. Misra and B. K. Bar, "Momentum integral method for studying flow characteristic of blood through stenosed vessel", *Biorheology*, 26, pp. 25–35, 1989.

[5] K. Haldar and S. N. Ghosh, "Effect of magnetic field on blood flow through indented tube in the presence of erythrocytes", *Ind. J. Pure Appl. Math.*, 25(3), pp. 345–352, 1994.

[6] V. P. Srivastava, "Particle –fluid suspension model of blood flow through stenotic vessels", *Int. J. Biomed. Comp.*, 38, pp. 141–154, 1995.

[7] H. P. Mazumdar, U. N. Ganguly and S. K. Venkatesan, "Some effects of magnetic field on flow of a Newtonian fluid through a circular tube", *Ind. J. Pure and Appl. Math.*, Vol. 5, pp. 519–524, 1996.

[8] Y. Haik, V. Pai and C. J. Chen, "Apparent viscosity of human blood in a high static magnetic field", *J. Magnetism and Magnetic Material*, Vol. 225, No. 14, pp. 180–186, 2001

[9] J. C. Misra and G. C. Shit, "Effect of magnetic field on blood flow through an artery: A numerical model", *J. Comput. Tech.*, Vol.12, No. 4, pp. 3–16, 2007.

[10] S. Kenjeres, S. "Numerical analysis of blood flow in realistic arteries subjected to strong non-uniform magnetic fields", *Int. J. Heat and Fluid Flow*, Vol. 29, No. 3, pp. 752–764, 2008.

[11] L. Parmar, S. B. Kulshreshtha and D. P. Singh, "The role of magnetic field intensity in blood flow through overlapping stenosed artery: A Herschel – Bulkley model", *Adv. Appl. Sci. Res.*, 4(6), pp. 318–328, 2013.

[12] M. Gaur and M. K. Gupta, "A Casson fluid model for the steady flow through a stenosed blood vessel", BJMCS, Vol. 4(11), pp. 1629–1641, 2014.

[13] M. Gaur and M. K Gupta, "Slip effects on steady flow through a stenosed blood artery", IJSER, Vol. 5, Issue 2, pp. 753–758, 2014.